



Egyptian Journal of Cell and Tissue Research

Print ISSN: 2812-5436 / Online ISSN: 2812-5444



Platelet-Rich Plasma Impact on Healing of Experimentally Induced Full-Thickness Skin Wound in Adult Male Albino Rats: Histological and Immunohistochemical Study

Marwa Mohamed Yousry*, Abeer Ibraheem Omar

*Histology Department, Faculty of Medicine, Cairo University, Cairo, Egypt**

Abstract:

Background: Failure to restore normal skin in slowly healed wounds as deep ones is a major health problem induced by deficient therapies. Platelet-rich plasma (PRP) is widely applied in different surgeries, diseases, regenerative medicine and skin youth rejuvenator. **Aim of work:** Evaluating PRP healing capabilities in experimentally full-thickness skin wound model in adult male rats. **Materials & Methods:** included 32 male albino rats (~3months,~200g); 8 for PRP preparation and 24 were subjected to full-thickness wound then divided equally into wounded-rat (group-I) and wounded-rat/PRP (group-II). Each was subdivided into two subgroups [Ia, Ib] & [IIa, IIb] according to their sacrifice at days 5 & 14. Biochemical [platelet-derived growth factor (PDGF) & transforming growth factor (TGF)- β], histological, immunohistochemical [vascular endothelial growth factor (VEGF), interleukin (IL)-1 α & CD-163] and statistical studies were done. **Results:** Skin PDGF, TGF- β levels and VEGF area-percent were increased in subgroups Ia & IIa versus control specimens and decreased in subgroups Ib & IIb versus Ia & IIa respectively. Subgroup Ia showed lost epidermis, numerous congested blood vessels, inflammatory cell infiltrate and absent skin appendages. In subgroup IIa the epidermis appeared with no skin appendages. Subgroup Ib illustrated epidermis, congested blood vessels, numerous inflammatory cells and no skin appendages. Subgroup IIb revealed apparently normal skin histological structure. Significantly increased IL-1 α and non-significantly increased CD-163

were recorded versus control sections in all subgroups except subgroup IIb. **Conclusion:** PRP could accelerate full-thickness wound healing and prevent scar formation via its anti-inflammatory and angiogenic abilities. besides, it promotes re-epithelialization, keratinocytes proliferation & proper collagen fibers arrangement.

Keywords: Full-thickness skin wound, PRP, VEGF, IL-1 α , CD-163

1. Introduction:

The skin is a protective barrier that provides an essential role in maintaining body fluid and electrolytes balance and protecting against pathogens invasion, radiation, physical and chemical injuries [1]. Such function is affected by the acute skin wound, especially the deep ones, induced by trauma, surgeries or burn [2]. Additionally, in association with certain diseases such as diabetes, or in cases of large extended wound or infection, the quality of tissue repair is affected, and the wound becomes chronic with ultimate pathological scar formation [3].

Skin wound is a major health problem despite the known cellular and molecular pathophysiology of healing in response to different injuries. Such crisis is caused by the lack of proper management for slowly healed wounds such as deep and chronic wounds even with the ideal healing conditions. This imperfect healing is followed by failure of restoration of normal skin structure and function with subsequent

major complications such as infection [4-6]. Therefore, it is eminent to speed up wound healing and regain the structural and functional skin integrity [7].

Platelet-rich plasma (PRP) is obtained from plasma via centrifugation of the whole blood. It is defined as an extract of plasma with platelet count higher than the normal levels in the peripheral blood [8].

Platelets are fragments of megakaryocytes cytoplasm which lack the nuclei [9]. They contain multiple types of granules one of them is α -granules which are thought to be the storage banks of platelets. These α -granules were proved to have abundance of multiple growth factors. Such growth factors include platelet-derived growth factor (PDGF), vascular endothelial growth factor (VEGF), epidermal growth factor (EGF), fibroblast growth factor (FGF), transforming growth factor- β (TGF- β), and insulin-like growth factor (IGF) [10]. Through these growth factors the platelets

can affect inflammation, angiogenesis, stem cell migration and cell proliferation [8].

Two principal methods are used for production of PRP: the PRP technique and the buffy-coat technique. In PRP method the whole blood is centrifuged at slow speed (soft spin) to isolate red blood corpuscles (RBCs). Then centrifugation of the supernatant plasma at higher speed (hard spin) to get the platelet concentrate. However, the buffy-coat method uses the whole blood which is prestored at 20-24°C. This is followed by hard spin centrifugation to separate the blood into 3 layers: RBCs, platelets, and white blood cells (WBCs), and platelet-poor plasma. The supernatant platelet-poor plasma is discarded, and the buffy-coat (platelets and WBCs) is isolated. Then the WBCs are separated either by centrifugation with a second soft spin or by using a leukocyte filter [11].

Initially, PRP was used as a transfusion product in patients suffering from thrombocytopenia [8]. Additionally, it has been widely used in numerous medical aspects including different fields of surgery such as plastic, pediatric, and cardiac surgeries as well as various aspects in gynaecology, urology and ophthalmology [12].

Moreover, PRP is considered now as an evolving technology in regenerative medicine, as its concentrated preparations are used to boost the natural healing process of the body [13]. So, it is widely used to renew and maintain skin youth by its ability to stimulate the regeneration of collagen type I in the dermis with subsequent partial or complete abolishing of the skin wrinkles [14].

Aim of work: Assessing the histological and immunohistochemical aspects of PRP abilities in healing of experimentally conducted full-thickness skin wound in adult male rats.

2. Materials & Methods:

I) Experimental Design

Thirty-two adult male albino rats (*Rattus rattus*) aged ~3 months, weighed ~200 g were utilized in the current study. The rats were maintained in Laboratory Animal House Unit of Kasr Al-Aini, Faculty of Medicine, Cairo University, fitting the instructions stated by the Institutional Animal Care and Use Committee (IACAUC), Cairo University [approval number CU/III/F/96/23]. Before starting the experiment, all rats were housed under the same environmental circumstances for 2 days to acclimatize to the new environmental situations. They were

supplied with regular chow and water *ad libitum* and kept at $24 \pm 1^\circ\text{C}$ in a normal light and dark cycle.

Eight rats were used for allogenic PRP preparation at Biochemistry Department, Faculty of Medicine, Cairo University, as follows: the rats were anesthetized using intramuscular injection of Ketamine [45 mg/kg] and Xylazine [20 mg/kg] ^[15]. Blood was withdrawn from inferior vena cava (3ml from each donor rat), collected in a tube with 3.8% sodium citrate and centrifuged to obtain PRP as follows: First centrifugation ($800 \times g$, 10 min) was used to separate the plasma. Then a second centrifugation ($1000 \times g$, 5 min) was used to concentrate the platelets in the plasma. ^[16]. The previously produced PRP was activated before use by addition of calcium chloride with a ratio of 1:10 (0.1 ml calcium chloride for every 1 ml PRP) ^[17]. The activated PRP contained a mean of $1,900,000 \pm 200,000$ platelets/ μL , whereas before the double centrifugation the platelets concentration was $410,000 \pm 28,000$ platelets/ μL .

The remaining 24 rats were subjected to full-thickness skin wounding ^[18], as follows:

Anaesthesia of the animals by intramuscular injection of Ketamine [45 mg/kg] and Xylazine [20 mg/kg] ^[15] was applied. Skin was disinfected by absolute

alcohol followed by shaving of hair. A permanent marker was used to localize the vertices of the square-shaped experimental wounds (2×2 cm dimensions) on the right dorsal side of each animal. Then, full-thickness skin specimen with its underlying subcutaneous tissue up to muscle layer was excised with a scalpel blade in each rat.

Pressure application with sterile cotton gauze was used to control any bleeding. This was followed by three days administration of Ampicillin antibiotic (50 mg/kg intraperitoneal injection) and Meloxicam anti-inflammatory (1 mg/kg subcutaneous injection) ^[19]. The exposed areas were dressed by Tegaderm (3M™ Tegaderm™ Non-Adherent Contact Layer 5642, USA) ^[20] for at least 24 hours to preserve the tissue fluid. After induction of wound, the rats were divided into two groups and each rat was housed singly in separate cages to avoid damage to their wounds.

Group I (wounded-rat group, 12 rats):

The animals of group I were further divided into 2 equal subgroups (Ia & Ib, 6 rats each) according to sacrifice time (5 days & 14 days, respectively).

Group II (wounded-rat/PRP group, 12 rats):

Animals of this group received local wound injection of activated PRP

immediately after induction of wound, in a dose of 250 µl/wound [21]. This dose was divided equally to 5 doses (50 µl each) and injected in 5 positions (12, 3, 6 & 9 O'clock and at the center of the wound) [21]. The rats were then divided according to time of sacrifice (5 days & 14 days) into two equal subgroups [IIa & IIb (6 rats each), respectively].

II) Animal studies

Gross observation of wounded rats' skin and estimation of wound closure:

Wounded skin of all rats was digitally photographed (iPhone 8 plus cell phone camera, dual 12-megapixel cameras). The size of wound closure was estimated at days 0,3,5,9 and 14. The unhealed area was measured by a millimetre graded ruler and evaluated using the formula, % of wound closure = [(wound size at 0 day – wound size of X days) /wound size at 0 day] × 100% [22].

Animals sacrifice:

At each time point (5 days & 14 days), The rats of the corresponding subgroup were sacrificed. This was done at the Laboratory Animal House Unit, where the animals were euthanized by Ketamine [45 mg/kg]/Xylazine [20 mg/kg] intramuscular injection [15]. Two full-thickness skin specimens after shaving of the hair were

obtained from each rat: one from the previously wounded area (right dorsal side) and the second one from the healthy skin on the left dorsal side of the animal's back (served as control skin for its subgroup to avoid variability in skin thickness between different rats for more accurate evaluation of the healing procedure). Each skin specimen (either from the control part or from the previously wounded part) was divided into two specimens one for biochemical studies [skin homogenate preparation & enzyme-linked immunosorbent assay (ELISA)] and one for paraffin blocks preparation.

III) Skin Homogenates and ELISA

Homogenization of skin were prepared at Biochemistry Department, Faculty of Medicine, Cairo University, respective to a previously described method [23]. This was followed by ELISA based on the manufacturer's instructions to measure the value of platelet-derived growth factor (PDGF) as well as transforming growth factor factor-β (TGF-β) using the suitable antibodies (MBS008389, MBS160117 respectively, MyBioSource, USA). PDGF, and TGF-β are growth factors included in α-granules of the platelets [8].

IV) Histological Study

Paraffin block preparation:

The skin of control and wounded specimens of animals of each subgroup were fixed in formol saline 10% and kept for twenty-four hours. Then, processing to paraffin blocks was performed. Skin sections of six µm-thick were sliced and stained with:

1- Hematoxylin and Eosin stain (H&E) ^[24]

to demonstrate the skin histological structure.

2- Masson's trichrome stain ^[24] for collagen fibers demonstration.

3- Immunohistochemical staining for:

Vascular endothelial growth factor (VEGF) [mouse monoclonal antibody,

ab1316, abcam, USA]: The most potent angiogenic mediator ^[25]. It is demonstrated as a cytoplasmic reaction ^[26] in cells producing VEGF as endothelial & inflammatory cells ^[7,27]. It is also expressed by keratinocytes following mechanical injury ^[28].

Interleukin-1α (IL-1α) [rabbit polyclonal antibody, PA5-89037, invitrogen, ThermoFisher Scientific, USA]: Proinflammatory cytokine ^[29], it is shown as cytoplasmic and nuclear reactivity ^[30] in the inflammatory cells, keratinocytes, endothelium, and fibroblasts ^[31].

Cluster of differentiation-163 (CD-163) [(EPR19518) rabbit monoclonal antibody,

ab182422, abcam, USA]: it is an indicator for macrophage anti-inflammatory phenotype (M2) that was illustrated as a positive reaction in the cytoplasm ^[32].

Using avidin-biotin technique, immunostaining was done ^[24]. Antigen retrieval was accomplished by boiling skin sections for 10 min in a 10 mM citrate buffer (cat no 005000) pH 6. Then, they were cooled at room temperature for 20 min. After that, the sections were incubated with the primary antibodies for 1 h. According to manufacturer's instruction, the recommended concentration was 5 µg/ml for VEGF, 1:50-1:200 for IL-1α and 1/500 for CD-163 antibodies. Immunostaining was performed using Ultravision One Detection System (cat no TL - 060- HLJ). Counterstaining was done by Lab Vision Mayer's hematoxylin (cat no TA- 060- MH).

The positive control sections for VEGF appeared as cytoplasmic immunoreaction in the rat's cerebellum and for IL-1α appeared as cytoplasmic and nuclear immunostaining in rat's lung. CD-163 positive control section illustrated as cytoplasmic positive immunoexpression in rat's liver. While the negative control sections were processed by the same steps after primary antibody exclusion.

Citrate buffer, Ultravision One Detection System and Ultravision Mayer's hematoxylin were purchased from Labvision, ThermoFisher Scientific, USA.

V) Morphometric study

Ten non-overlapping fields ($\times 400$) were taken from the six animals as follows six sections from the control side (left side) and six sections from the wounded area (right side) in each subgroup, for assessment of the following items:

- The total thickness of epidermis in H&E-stained sections.
- The area percent of collagen deposition in Masson's trichrome-stained sections
- The area percent of VEGF positive immun-expression in anti-VEGF immunostained sections.
- The area percent of the positive immunostaining for IL-1 α in anti-IL-1 α immunostained sections.
- The number of CD-163 positive immunostained cells in anti-CD-163 immunostained sections.

Image analysis was performed using Leica Qwin-500 LTD-software image analysis computer system (Cambridge, England).

All the histological and morphometric studies were done at the Department of

Histology, Faculty of Medicine, Cairo University.

VI) Statistical analysis ^[33]

The biochemical as well as morphometric measurements were presented as mean \pm standard deviation (SD). They were statistically analyzed by one-way analysis of variance (ANOVA) and then "Tukey" post hoc test. Wound closure percentage was statistically analyzed using independent samples T-test. This was performed using IBM Statistical Package for the Social Sciences (SPSS) version 21. The findings appeared significant at P value < 0.05.

3. Results:

General observations

Neither deaths nor abnormal behaviour were noticed in any of the experimental rats.

The control skin specimens (left dorsal side) in rats of all subgroups showed nearly the same biochemical & histological results. Thus, they were called as the control specimens.

Animal Data

Results of gross evaluation of rat's skin wounds [Figs. 1a-1j]:

This was assessed on days 0, 3, 5, 9, and 14 in untreated rats [Figs. 1a-1e]. After three days, the untreated rats developed hyperaemic wounded area. At day 5, the

wound was covered with a dry crust. At day 9 the crust was reduced and visible at wound margins, the wounded area was covered by granulation tissue. At day 14, the wound size was clearly decreased and covered by scar with only a small area of delayed closure. However, in PRP-treated [Figs. 1f-1j], the wounds were entirely covered by crust at day 3. This was followed by appearance of healthy moist granulation tissue and parts of crust at wound margins at day 5. An apparent decrease in wound diameter was observed from day 5, until an obvious wound reduction at day 9 and complete closure with apparently normal skin at day 14.

Wound closure percentage results [Fig. 1k]:

Intradermal injection of PRP significantly enhanced the mean wound closure percentage versus untreated rats at days 5, 9 and 14.

ELISA Results for PDGF and TGF- β [Fig. 2]:

Subgroups Ia & IIa revealed significant increase in comparison to control specimens however subgroups Ib & IIb showed non-significant increase versus the control skin. In addition, subgroups Ib & IIb showed significant decrease versus subgroups Ia & IIa, respectively. Moreover, subgroup IIa

demonstrated significant increase in comparison to subgroup Ia whereas subgroup IIb revealed non-significant increase versus subgroup Ib.

Histological Results:

H&E-stained sections

Control sections [Fig. 3a]:

Histologically the sections appeared with normal structure of thin skin (epidermis & underlying dermis). Epidermis, keratinized stratified squamous epithelium, represented the outermost part of the skin, and formed of 4 layers: stratum basale, stratum spinosum, stratum granulosum & stratum corneum. Stratum basale (basal cell layer) rested on a clear basement membrane. Its cells were arranged in a single row and seemed like cuboidal cells with basophilic cytoplasm and basal nuclei. Stratum spinosum (the prickle cell layer) was the second layer that described most of the epidermal thickness. It was composed of many layers of polyhedral cells with oval to rounded nuclei and prominent nucleoli. Stratum granulosum or the granular cell layer was the third layer that was formed of squamous cells with flattened nuclei and basophilic granules arranged in several layers. The fourth and the most superficial stratum was the stratum corneum (the horny layer). It revealed keratinized acidophilic interwoven non-

cellular layer. Next to the skin epidermis was the dermis, the thick connective tissue layer beneath the epidermal basement membrane. It demonstrated thick bundles of collagen fibers which were closely packed together and variably oriented, blood vessels and different appendages of skin (hair follicles & sebaceous glands) in addition to erector pili muscle.

Subgroup Ia [Fig. 3b]:

The skin sections of the wounded rats after 5 days revealed absence of the superficial epidermis with crust formation. In addition, there was cellular tissue with numerous congested blood vessels, multiple mononuclear inflammatory cell infiltrate and no skin appendages.

Subgroup Ib [Fig. 3c]:

The skin sections of the wounded rats after 14 days demonstrated epidermal wound cover, frequent congested blood vessels and numerous inflammatory cells. No skin appendages were observed.

Subgroup IIa [Fig. 3d]:

Examination of skin sections of the wounded rats 5 days after receiving PRP showed epidermal cells with the presence of crustation. Underlying the epidermis there was high cellularity with numerous blood vessels. In addition, to the presence of multiple inflammatory cellular infiltrates.

The skin appendages were not detected. The adjacent normal skin showed thick collagen bundles in the CT dermis.

Subgroup IIb [Fig. 3e]:

After 14 days of PRP treatment, the wounded area showed nearly normal epidermis and dermis which revealed blood vessels, few inflammatory cells and many hair follicles, sebaceous glands and erector pili muscle.

Masson's trichrome-stained sections

The control rats' skin sections [Fig. 4a] exhibited a network of interwoven bundles of thick collagen fibers organized in various directions. In subgroup Ia [Fig. 4b] the collagen bundles were scanty and thin. In subgroup Ib [Fig. 4c], the collagen bundles appeared thin and organized in one direction. With PRP treatment, there were relatively more collagen bundles following 5 days in subgroup IIa [Fig. 4d] as compared to subgroup Ia. While after 14 days of the PRP treatment in subgroup IIb [Fig. 4e], densely packed thickened collagen bundles interlaced in variable directions forming a reticulum were detected.

VEGF immunostained sections

The negative control skin sections [Fig. 5a]: showed negative immunostaining in skin tissue after omitting the adding of VEGF primary antibody.

Control sections [Fig. 5b]:

The positive cytoplasmic immunoreactivity was noted in few endothelial cells lining the dermal blood vessels and in few mononuclear inflammatory cells in the dermis.

Subgroup Ia [Fig. 5c]:

There was positive immunostaining in the endothelium lining the blood vessels and inflammatory cells after 5 days.

Subgroup Ib [Fig. 5d]:

After 14 days, the immunopositivity was visualized in the endothelium lining the dermal blood vessels, inflammatory cells and keratinocytes.

Subgroup IIa [Fig. 5e]:

The skin specimens after 5 days demonstrated widespread positive immunoreaction in the endothelium of blood vessels and mononuclear inflammatory cells. As well as keratinocytes exhibited positive immune expression for VEGF.

Subgroup IIb [Fig. 5f]:

After 14 days, the immunoreactivity was minimally detected in the blood vessels endothelial cells and in few inflammatory cells.

IL-1 α immunostained sections

In the negative control skin sections [Fig. 6a] with skipping the step of IL-1 α primary

antibody, a negative immunostaining was illustrated.

Control sections [Fig. 6b]:

The positive immunoreaction was scarcely spread throughout the cytoplasm and/or nuclei of the few keratinocytes, dermal inflammatory cells, fibroblast-like cells and endothelial cells.

Subgroup Ia [Fig. 6c]:

Confirmed immunopositive reaction in the inflammatory cells, fibroblast-like cells and endothelial cells.

Subgroup Ib [Fig. 6d]:

Showed widely distributed positive reaction in keratinocytes, dermal inflammatory cells, fibroblast-like cells and endothelial cells.

Subgroup IIa [Fig. 6e]:

Revealed positive immunoreactivity in some keratinocytes, multiple inflammatory cells, fibroblast-like cells and endothelium lining dermal blood vessels.

Subgroup IIb [Fig. 6f]:

The positive immunoreaction was detected in few keratinocytes, dermal inflammatory cells, fibroblast-like cells and endothelial cells.

CD-163 immunostained sections

Negative control sections of skin specimen [Fig. 7a] exhibited negative immunostaining

with overstep the application of CD-163 primary antibody.

Control sections [Fig. 7b]:

Showed few positive immune reactions in the dermal inflammatory cells.

Subgroup Ia [Fig. 7c]:

CD-163 immunoreactivity was detected in few inflammatory cells.

Subgroup Ib [Fig. 7d]:

The positive immunoreactivity was seen in few dermal inflammatory cells.

Subgroup IIa [Fig. 7e]:

Few CD-163 immunoreactivity was noted in the inflammatory cells.

Subgroup IIb [Fig. 7f]:

Multiple CD-163 immunopositive inflammatory cells were detected throughout the dermis.

Morphometric Results:

Epidermal thickness (Fig. 3f):

Subgroup Ia demonstrated absent epidermis. Statistically, subgroups Ib & IIa revealed significant decrease versus control section while subgroup IIb showed non-significant decrease versus the control skin. Moreover, subgroup IIb was significantly increased compared to both subgroups Ib & IIa.

Mean area percent of collagen fibers (Fig. 4f):

All subgroups revealed significant decrease versus the control skin except subgroup IIb that showed insignificant decrease. Subgroups Ib & IIa demonstrated significant increase compared to subgroup Ia. Additionally, subgroup IIb showed significant rise relative to subgroups Ib & IIa.

Mean area percent of VEGF immunopositive cells (Fig. 5g):

There was statistically significant elevation in all subgroups versus the control section. Moreover, subgroups Ib & IIb showed significant decrease versus subgroups Ia & IIa, respectively. Furthermore, subgroup IIa demonstrated significant boost versus subgroup Ia, however subgroup IIb revealed non-significant decrease compared to subgroup Ib.

Mean area percent of IL-1 α immunopositive cells (Fig. 6g):

There was significant rise in all subgroups in comparison to the control skin except in subgroup IIb that recorded non-significant increase versus the control section. In addition, subgroup Ib illustrated significant elevation versus subgroup Ia while subgroup IIb revealed significant reduction versus subgroup IIa. Additionally, subgroup IIa demonstrated significant

increase in comparison to subgroup Ia. Furthermore, subgroup IIb revealed significant decrease versus subgroup Ib.

Mean number of CD-163 immunopositive cells (Fig. 7g):

The number of CD-163 immunopositive cells elevated non-significantly in all subgroups in comparison with the control

section except subgroup IIb that demonstrated significant rise versus the control skin. Moreover, the number of CD-163 raised non-significantly in subgroups Ib & IIa versus subgroup Ia. Besides, there was significant increase in subgroup IIb versus subgroups IIa & Ib.

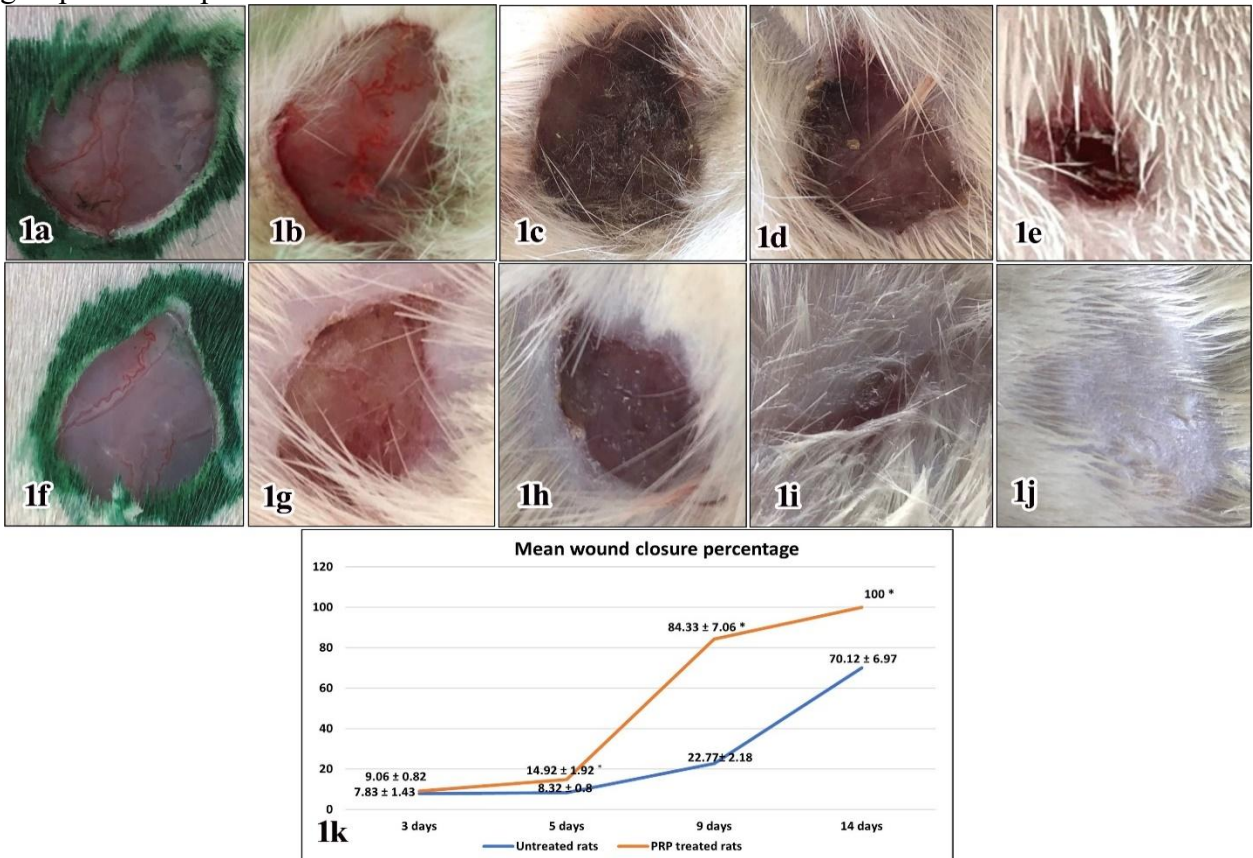


Figure 1: Photographs of gross wound evaluation illustrating:

1a,1b,1c,1d&1e of untreated wounded skin at day 0,3,5,9&14 respectively.

1a: at day 0; skin wound.

1b: at day 3; hyperaemic wound.

1c: at day 5; The wound is covered with a dry crust.

1d: at day 9; granulation tissue appears, and the crust is noticed at the wound margins.

1e: at day 14; wound size is clearly decreased and covered by scar, with just a small part showing delayed closure.

1f, 1g,1h,1i&1j of PRP treated wounded skin at day 0,3,5,9&14 respectively.

1f: at day 0; skin wound.

1g: at day 3; wound is completely covered by crust.

1h: at day 5; the wound is entirely covered with healthy moist granulation tissue, with parts of crust visible at the wound borders.

1i: at day 9; a small wound area is visible.

1j: at day 14; complete wound closure with apparently intact skin.

1k: The mean values of wound closure percentage. [* as compared to untreated wounded skin (significant difference at $P < 0.05$)]

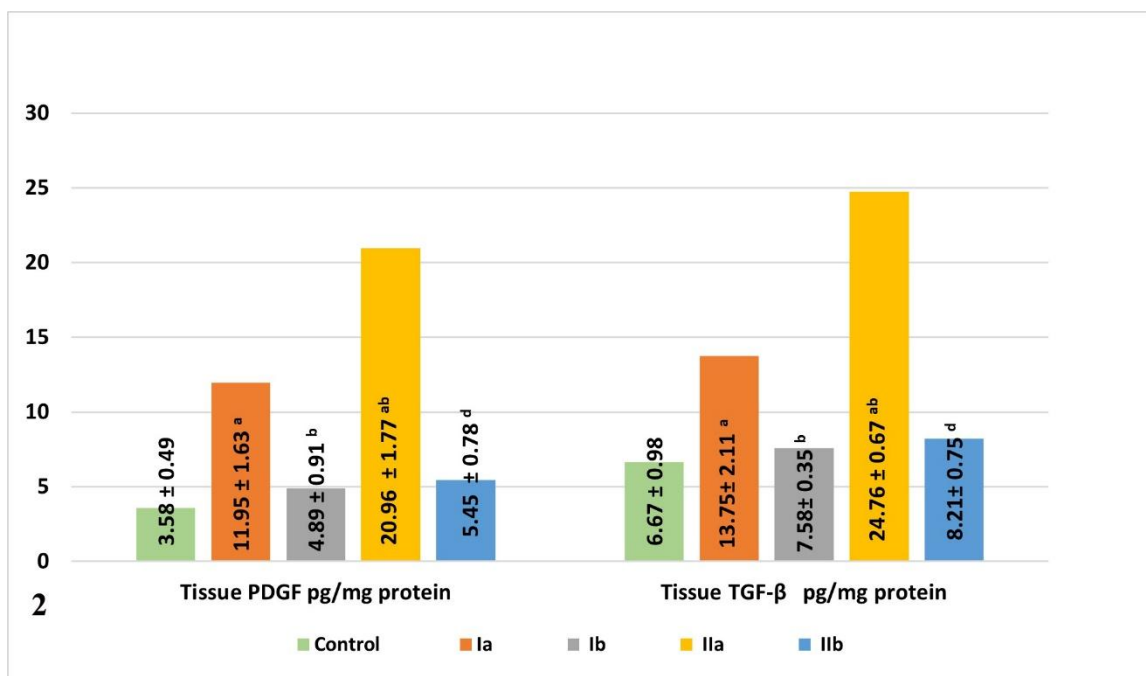


Figure 2: Showing mean values of: skin homogenate PDGF and TGF-β levels.

[^a as compared to control specimen, ^b as compared to subgroup Ia, & ^d as compared to subgroup IIa (significant difference at $P < 0.05$)]

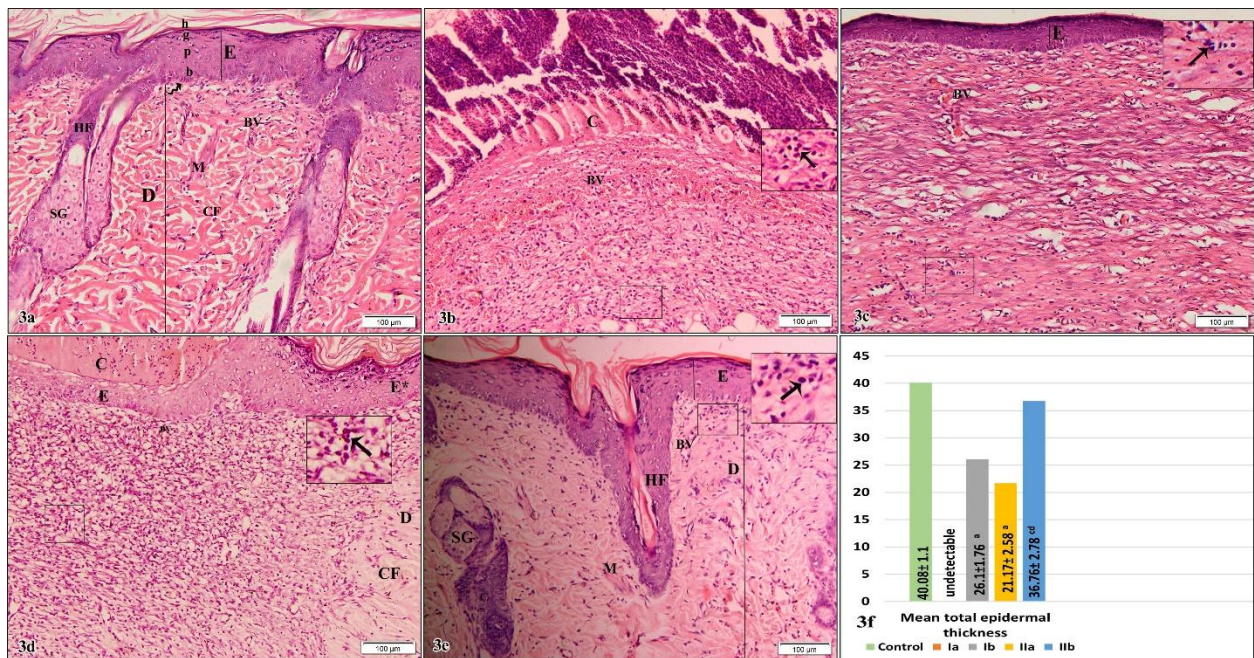


Figure 3: Photomicrographs of H&E-stained skin sections of:

3a (The control section): Showing normal structure of thin skin formed of epidermis (E) and dermis (D). The epidermis is consisted of 4 layers: basal cell layer (b); one row of cuboidal cells with basal nuclei rested on the basement membrane (wavy arrow), prickle cell layer (p); many layers of polyhedral cells with rounded to oval nuclei and prominent nucleoli, granular cell layer (g); flattened cells with flattened nuclei and basophilic granules, and horny layer (h); acidophilic interwoven non-cellular layer. The dermis illustrates variably oriented, thick bundles of collagen fibers (CF), blood vessels (BV), hair follicles (HF), sebaceous gland (SG) and erector pili muscle (M).

[H&E, x100]

3b (Subgroup Ia, wounded-rat after 5 days): Demonstrating lost superficial epidermis with the presence of crust (C). In addition, high cellularity with numerous congested blood vessels (BV), multiple mononuclear inflammatory cells (arrow) and lost skin appendages are observed.

[H&E, x100, inset x200]

3c (Subgroup Ib, wounded-rat after 14 days): Showing epidermis (E), frequent dermal congested blood vessels (BV) as well as numerous inflammatory cells (arrow) in addition to absence of skin appendages.

[H&E, x100, inset x200]

3d (Subgroup IIa, wounded-rat/PRP after 5 days): Illustrating crust (C) and epidermal cells (E) covering the wound bed. The underling tissue appears highly cellular with multiple blood vessels (BV), and multiple inflammatory cellular infiltration (arrow). The skin appendages are not detected.

Part of adjacent normal skin is noticed formed of epidermis (E*) and dermis (D) having thick collagen bundles (CF).

[H&E, x100, inset x200]

3e (Subgroup IIb, wounded-rat/PRP after 14 days): Showing nearly normal epidermis (E) and dermis (D) with blood vessels (BV), few inflammatory cells (arrow) and multiple hair follicles (HF), sebaceous glands (SG) and erector pili muscle (M).

[H&E, x100, inset x200]

3f: Showing the mean values of the total epidermal thickness. [^a as compared to control section, ^c as compared to subgroup Ib & ^d as compared to subgroup IIa (significant difference at $P < 0.05$)]

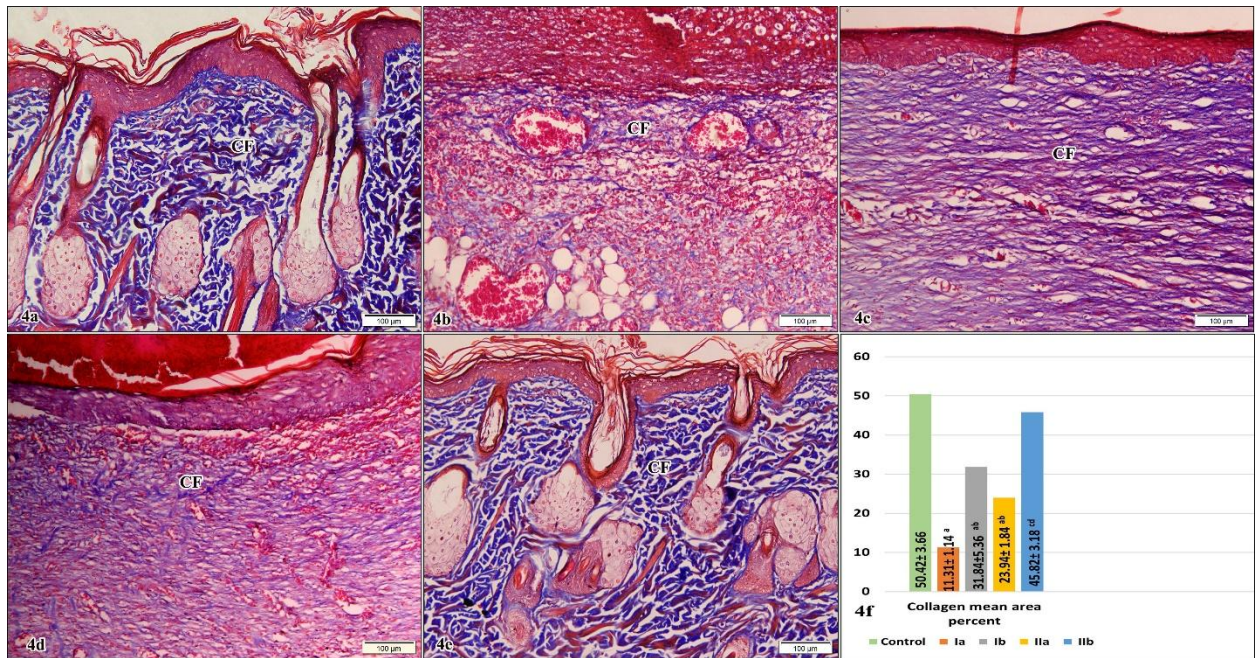


Figure 4: Photomicrographs of Masson's trichrome-stained sections of skin of:

4a (The control section): Interlacing closely packed blue stained thick bundles of collagen fibers (CF) arranged in variable directions are noticed.

[Masson's trichrome stain, x100]

4b (Subgroup Ia, wounded-rat after 5 days): Collagen bundles (CF) appear thin and scanty.

[Masson's trichrome stain, x100]

4c (Subgroup Ib, wounded-rat after 14 days): Demonstrating thin collagen bundles (CF) arranged in one direction.

[Masson's trichrome stain, x100]

4d (Subgroup IIa, wounded-rat/PRP after 5 days): Showing relatively multiple collagen bundles (CF) as compared to subgroup Ia (fig. 4b).

[Masson's trichrome stain, x100]

4e (Subgroup IIb, wounded-rat/PRP after 14 days): Interwoven closely packed thick collagen bundles (CF) are seen run in different directions creating a network.

[Masson's trichrome stain, x100]

4f: Demonstrating the mean area percent of collagen fibers. [^a as compared to control section, ^b as compared to subgroup Ia, ^c as compared to subgroup Ib & ^d as compared to subgroup IIa (significant difference at $P < 0.05$)]

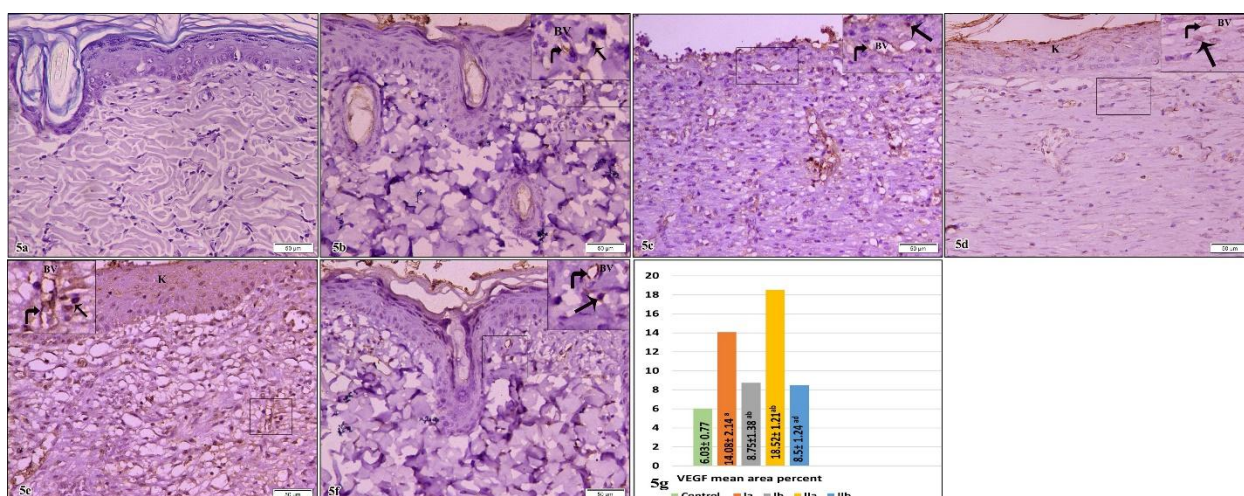


Figure 5: Photomicrographs of anti-VEGF immunohistochemically stained skin sections of:
5a negative control skin section with skipping the VEGF primary antibody showing negative immunostaining.

[x200]

5b (The control section): Demonstrating positive cytoplasmic immunoreaction in few endothelial cells (right angle arrow) lining the dermal blood vessels (BV) and few inflammatory cells (straight arrow).

[anti VEGF immunohistochemical stain, x200, inset x400]

5c (Subgroup Ia, wounded-rat after 5 days): The positive immunoreaction is noticed in the endothelium (right angle arrow) lining the blood vessels (BV) and mononuclear inflammatory cells (straight arrow).

[anti VEGF immunohistochemical stain, x200, inset x400]

5d (Subgroup Ib, wounded-rat after 14 days): Showing positive immunoreactivity in the dermal blood vessels (BV) endothelial cells (right angle arrow) and inflammatory cells (straight arrow), as well as in the keratinocytes (K).

[anti VEGF immunohistochemical stain, x200, inset x400]

5e (Subgroup IIa, wounded-rat/PRP after 5 days): Abundant positive immunoreactivity in endothelial cells (right angle arrow) lining the blood vessels (BV) and inflammatory cells (straight arrow) are observed. Positive immunostaining in epidermal keratinocytes (K) is detected.

[anti VEGF immunohistochemical stain, x200, inset x400]

5f (Subgroup IIb, wounded-rat/PRP after 14 days): Illustrating few immunoreactive endothelial cells (right angle arrow) lining the dermal blood vessels (BV) and inflammatory cells (straight arrow).

[anti VEGF immunohistochemical stain, x200, inset x400]

5g: Demonstrating the mean area percent of VEGF positive reaction. [^a as compared to control section, ^b as compared to subgroup Ia & ^d as compared to subgroup IIa (significant difference at $P < 0.05$)]

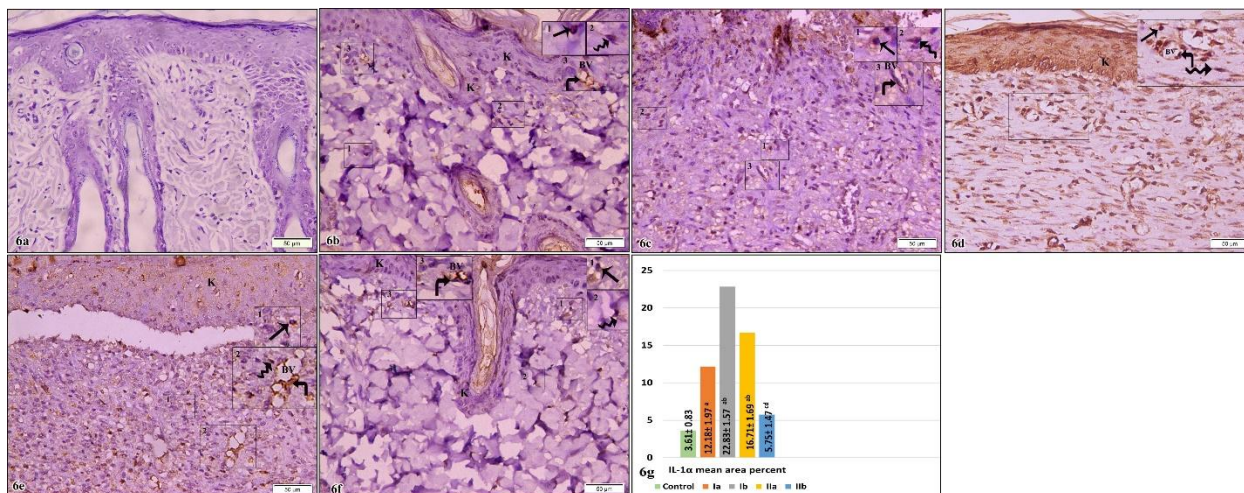


Figure 6: Photomicrographs of anti-IL-1 α immunohistochemically stained skin sections of: 6a the negative control skin section after omitting the IL-1 α primary antibody illustrating negative immunostaining.

[x200]

6b (The control section): Cytoplasmic and/or nuclear immunoreaction is seen in very few keratinocytes (K), dermal inflammatory cells (straight arrow), fibroblast-like cells (wavy arrow) and endothelium (right angle arrow) lining blood vessels (BV).

[anti IL-1 α immunohistochemical stain, x200, insets 1,2&3 x400]

6c (Subgroup Ia, wounded-rat after 5 days): Immunopositive reaction is detected in the inflammatory cells (straight arrow) as well as fibroblast-like cells (wavy arrow) and endothelium (right angle arrow) lining blood vessels (BV).

[anti IL-1 α immunohistochemical stain, x200, insets 1,2&3 x400]

6d (Subgroup Ib, wounded-rat after 14 days): Illustrating widely spread immunoreactivity in numerous keratinocytes (K), inflammatory cells (straight arrow), fibroblast-like cells (wavy arrow) and endothelial cells (right angle arrow) lining dermal blood vessels (BV).

[anti IL-1 α immunohistochemical stain, x200, inset x400]

6e (Subgroup IIa, wounded-rat/PRP after 5 days): The positive immunoreaction is detected in some keratinocytes (K), multiple inflammatory cells (straight arrow), in addition to fibroblast-like cells (wavy arrow) and endothelium (right angle arrow) of dermal blood vessels (BV).

[anti IL-1 α immunohistochemical stain, x200, insets 1&2 x400]

6f (Subgroup IIb, wounded-rat/PRP after 14 days): There is few positive immunoreaction in the keratinocytes (K), inflammatory cells (straight arrow), fibroblast-like cells (wavy arrow) and endothelium (right angle arrow) lining blood vessels (BV).

[anti IL-1 α immunohistochemical stain, x200, insets 1,2&3 x400]

6g: Demonstrating the mean area percent of IL-1 α positive reaction. [^a as compared to control section, ^b as compared to subgroup Ia, ^c as compared to subgroup Ib & ^d as compared to subgroup IIa (significant difference at $P < 0.05$)]

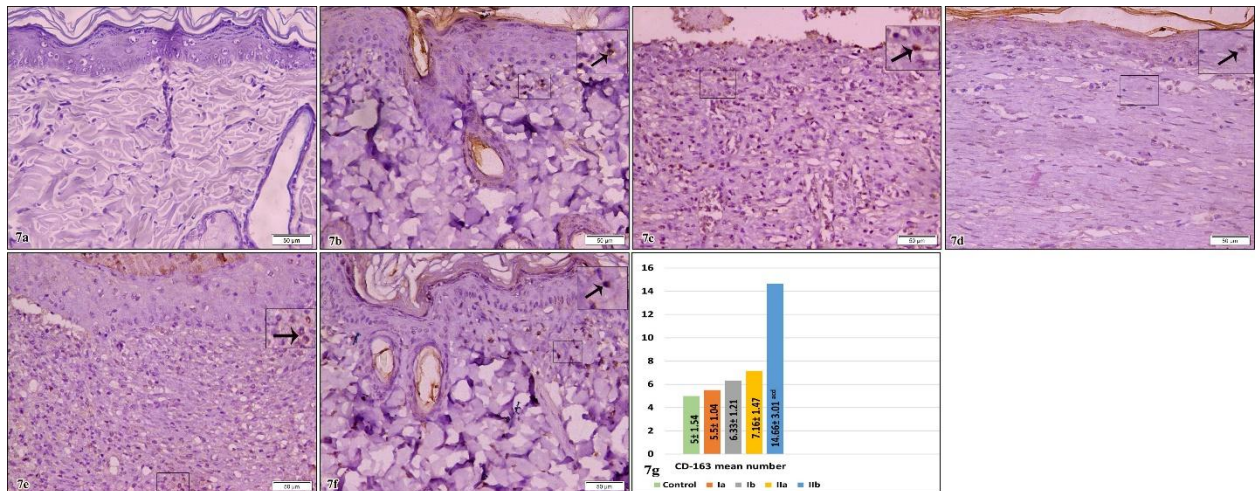


Figure 7: Photomicrographs of anti-CD-163 immunohistochemically stained skin sections of:
7a negative control skin section: Demonstrating negative immunostaining after skipping the addition of the CD-163 primary antibody.

[x200]

7b (The control section): Showing cytoplasmic positive immunoreactivity in few inflammatory cells (straight arrow).

[anti CD-163 immunohistochemical stain, x200, inset x400]

7c (Subgroup Ia, wounded-rat after 5 days), 7d (Subgroup Ib, wounded-rat after 14 days) and 7e (Subgroup IIa, wounded-rat/PRP after 5 days): The immunoreactivity is seen in few inflammatory cells (straight arrow).

[anti CD-163 immunohistochemical stain, x200, inset x400]

7f (Subgroup IIb, wounded-rat/PRP 14 days): Many CD-163 immunopositive inflammatory cells (straight arrow) are observed.

[anti CD-163 immunohistochemical stain, x200, inset x400]

7g: Demonstrating the mean number of CD-163 positive reaction. [a as compared to control section, c as compared to subgroup Ib & d as compared to subgroup IIa (significant difference at $P < 0.05$)]

4. Discussion:

This study targeted at assessing histological and immunohistochemical aspects of PRP abilities in repair of experimentally conducted full-thickness skin wound in adult male rats.

A previous methodology ^[18] was used to apply the full-thickness skin wound as it allowed easy performance of a precise wound. Moreover, the specimens of the control skin were obtained from the same wounded-rats in each subgroup to provide proper assessment of the healing process.

In this work, PRP was chosen as it was easily obtained from the venous blood by centrifugation. It was prepared from the rat's donor blood (Allogenic PRP) being safe from adverse immune reactions ^[34]. In addition, its activation by calcium chloride was documented to achieve high amounts of platelets' growth factors and cytokines such as PDGF, VEGF, TGF- β , FGF & IGF-1^[35]. This was illustrated in the current study by the significant increase in the mean value of PDGF along with TGF- β in skin homogenate and the mean area percent of VEGF on day 5 in subgroup IIa (PRP-treated) versus the control skin. Such growth factors resulted into widespread use of PRP in different surgical operations and clinical protocols of treatment ^[36-39].

Additionally, in this study the dose of the activated PRP was divided into 5 equal portions and applied topically via injectable route ^[21]. This was assumed to achieve equal distribution of high PRP concentration all around the wounded area. So, maximum PRP effect and proper evaluation of the results were obtained.

Skin wound healing is based on multiple major pillars: haemostasis, coagulation, inflammation, angiogenesis, formation of granulation tissue, deposition of collagen and re-epithelialization ^[40].

Coagulation likewise haemostasis was proved to occur immediately after an acute skin wound via release of the clotting factors from the injured tissues with subsequent platelet activation, aggregation and clot formation ^[41,42]. This was demonstrated grossly by the detection of skin crustation in the present study 5 days after wound induction in untreated rats and 3 days in PRP-treated rats. This is in line with previous studies after induction of full-thickness skin wound in mice ^[7,43].

Bearing in mind that the early and basic step of tissues defence against injury is by inflammation as it is very crucial to the entire wound curing process ^[44] where inflammation provides an immunological barrier that prevents entry of pathogenic organisms and phagocytoses the invading

ones with removal of cell debris, and damaged tissue. In addition, the optimum inflammatory response is divided into two stages [early and late stages] ^[45]. The early stage occurs as early as the first 5 days where neutrophils and monocytes are the predominating cells in the first 24-36 hours ^[46] and macrophages become the main inflammatory cells from the 2nd to the 5th day after wound induction ^[47]. While during the late stage of inflammation (till day 14), macrophages decrease gradually ^[48]. Such macrophages have two phenotypes: classically stimulated pro-inflammatory M1 and alternatively stimulated anti-inflammatory M2 ^[45,49].

In this work during the early stage of inflammation (day 5) in subgroup Ia, the platelets activated by the mediators released from the damaged tissues were suggested to release growth factors like PDGF & TGF- β 1. Such factors could attract neutrophils and macrophages to the wound site ^[50]. This suggestion could explain the significant rise in the mean value of PDGF and TGF- β , the congested dilated blood vessels and the inflammatory cell infiltration noticed in this subgroup versus the control section.

The activated platelets were stated to attract M1 to the site of wound during the early stage of inflammation ^[7]. M1 macrophages, in turn, increased the synthesis of IL- α & IL- β in addition to other proinflammatory factors such as IL-6, along with tumour

necrosis factor alpha and beta (TNF- α & TNF- β) ^[51,52,53] to speed up the initial stage of wound healing ^[52]. This could clarify the significant elevation in the mean area percent of IL-1 α detected in subgroup Ia of this study versus the control skin. In addition, it could furtherly support the increase in inflammatory cells in this subgroup versus the control section.

During the early phase of inflammation in the PRP-treated subgroup IIa there was significant boost in the mean values of PDGF and TGF- β , numerous inflammatory infiltrations, multiple blood vessels, and significant rise in the mean area percent of IL-1 α relative to subgroup Ia. Such findings could be enlightened by the higher amount of the activated platelets in this subgroup as they were provided from the PRP in addition to those activated endogenously. More activated platelets resulted into more PDGF and TGF- β with subsequent attraction for more inflammatory cells and M1 macrophages and more production of IL-1 α . Similarly, an increase in levels of PDGF, TGF- β and IL-1 β mRNA expression was noticed in previous study in PRP treated group compared to antibiotic treated wound group on days 3 and 7 ^[15]. Further support was illustrated formerly where increased macrophages infiltration was observed 7 days following PRP administration in wounded rats ^[54].

In subgroups Ib & IIb (sacrificed at day 14), there were significant decrease in PDFG and TGF- β mean value in the skin homogenate versus subgroups Ia & IIa, respectively. In addition, it showed non-significant elevation in these two subgroups compared to the control section and non-significant increase in subgroup IIb versus subgroup Ib. This was suggested by that PDGF and TGF- β are released from alpha granules of the platelets only following their activation [55]. And the platelets were proved to have life span of ~5 days [56]. This is in line with observation of prior authors where they detected TGF- β decline reaching minimal 14 days of wound [57]. Similarly, a decrease in PDGF and TGF- β expression 14 days following PRP treatment in full thickness wound model was reported [15]. Bearing in mind the fact stated that for proper healing process to occur, there must be a balance between anti-inflammatory and pro-inflammatory mediators in the inflammatory response. So, moderate inflammation is helpful while excess inflammation is hurtful to wound healing [58]. This fact could be achieved by the switch of pro-inflammatory M1 to anti-inflammatory M2 that occurred at 5-7 days after injury where M2 cells gradually dominate the wound sites [59,60]. This shift was not detected in subgroup Ia & IIa of this work where the mean number of CD-163 (specific

M2 marker) showed non-significant rise in these two subgroups compared to the control skin and in subgroup IIa versus Ia. Such transition was reported to occur following proper elimination of wound debris and pathogens by the inflammatory cells during the acute inflammatory stage [achieved by numerous proinflammatory M1] [61]. Moreover, it is followed by secretion of M2 anti-inflammatory cytokines as TGF- β 1 [53] with subsequent gradual decrease in the inflammatory cell infiltrating the site of wound [shift from the numerous proinflammatory M1 to fewer anti-inflammatory M2] [48].

In subgroup Ib, there was congested blood vessels, more abundant inflammatory cells with significant elevation in the mean area percent of IL-1 α immunoreactivity in inflammatory cells, keratinocytes, endothelium, and fibroblast-like cells versus subgroup Ia. This is in accordance with prior study where it hypothesized that IL-1 α is increased after skin injury and during chronic inflammation of skin and is expressed by keratinocytes [62].

This finding was assumed to be due to unregulated inflammatory response and improper cleaning of the wound during the acute inflammatory stage by the inflammatory cells with no transition of M1 cells to M2 cells state enforced by non-significant rise in mean number of CD-163

detected in subgroup Ib versus the control section and subgroup Ia.

But in subgroup IIb, it was assumed that there was efficient cleaning of the wound during the acute inflammatory stage with subsequent shift of proinflammatory M1 state to anti-inflammatory M2 state that was followed by production of anti-inflammatory cytokines and subsequent decrease in the inflammatory cell infiltration. This assumption was reinforced by the significant rise in the mean number of CD-163 in this subgroup in comparison to control section and subgroups IIa & Ib.

In addition to the obvious reduction of the inflammatory cells and the non-congested blood vessels detected at the wound site of subgroup IIb to the extent that was similar to the normal condition. Besides, IL-1 α mean area percent in this subgroup revealed a significant lower value than subgroups IIa & Ib and non-significant increase compared to the control skin. This suggestion was similarly recorded in former research [7] where the full-thickness skin wound treated with PRP showed marked reduction in the number of M1 macrophages & the inflammatory process and increased M2:M1 ratio from the 7th day of wound induction in comparison to the untreated wound. Further support came from another study that reported the efficacy of PRP in decreasing the extent of wound inflammation and IL-1 β [15,43] & IL-17 inflammatory cytokine

production [43]. Therefore, PRP anti-inflammatory effect might contribute to modulate the process of wound healing.

VEGF is another growth factor concerned with proliferation of the endothelial cells and angiogenesis via its binding to its receptors on the endothelial cells [63,64]. Angiogenic response is pivotal for healing of wound, and is essential to elevate oxygen and nutrient delivery, to sustain keratinocytes survival, and maintain the formation of granulation tissue [54]. VEGF is released from α -granules of the platelets only when they are activated similar to PDGF and TGF- β [7,10]. In addition, the platelets were proved to have life span of ~5 days [56]. Moreover, there was more activated platelets in subgroup IIa (PRP-treated subgroup) versus Ia (non-treated subgroup).

There was increased blood vessels content and significant rise in the mean area percent of VEGF in subgroup Ia versus the control section and in subgroup IIa versus Ia. This was illustrated as positive cytoplasmic reactions in endothelial cells, inflammatory cells, in addition to keratinocytes that showed positive immunostaining during wound repair as reported previously [28]. Similar results were recorded previously in mice 5 days following full-thickness skin wound induction [43]. However, VEGF area percent revealed significant decrease in the

current study in subgroups Ib & Iib in comparison to subgroups Ia & Iia, respectively and significant increase in subgroups Ib & Iib versus control skin and non-significant decrease in subgroup Iib versus Ib. The transcription of VEGF was raised shortly after wound induction till day 7. Then it is reduced, reaching lower values on day 14 ^[57]. This was illustrated by former researchers. They recorded decreased blood vessels 15 days after wound induction following PRP hydrogel-treatment ^[65]. This was explained by remodeling phase where blood vessels form mature vessel structures with perfect functions, while the immature vessels disappeared ^[66].

A third growth factor produced from the α -granules of the activated platelets is TGF- β 1 ^[10]. Such factor is responsible for fibroblasts proliferation with subsequent collagen production ^[53]. This was supported in the present work by the significant rise in mean value of TGF- β along with the abundant cellular tissue detected on the 5th day of the experiment (early inflammatory stage) in subgroups Ia & Iia versus the control specimens.

Such high cellularity together with high blood vessels content induced by VEGF form the protective granulation tissue which is highly resistant to infection. Moreover, it provides a surface for the epithelial cells to creep from the periphery of the wound to cover it ^[67]. More support came from the

more collagen fibers produced by the proliferated fibroblasts in subgroup Iia than Ia but its mean area percent showed significant decrease versus the control section. Additionally, the significant elevation in such area percent of subgroup Iia versus subgroup Ia could be explained by the production of more TGF- β 1 from the more activated platelets provided by PRP in subgroup Iia than the untreated subgroup Ia. Similar results were recorded in previous studies where collagen deposition and its statistical analysis revealed significant increase in the PRP-treated animals versus the untreated animals following full-thickness wound induction in mice by 5 days ^[43] and in wounded rats by 7 days ^[35].

In the late inflammatory stage (subgroups Ib & Iib), the fibroblasts were assumed to continue production of collagen bundles with consequent rise in its mean area percent in subgroups Ib & Iib versus subgroups Ia & Iia, respectively. However, the collagen bundles in subgroup Iib showed significant boost in its mean area percent as compared to subgroup Ib and non-significant reduction relative to the control skin. In addition to the proper interwoven densely packed arrangement demonstrated in this subgroup when compared to subgroup Ib. These findings coincided with the results reported in former studies 12 days ^[68] and 14 days ^[69] following treatment

with PRP versus the untreated wound. Such finding could be clarified by the significant presence of M2 cells in subgroup IIb versus Ib with continuation of TGF- β 1 production [53]. The proper deposition and arrangement of the collagen fibers in the wound area promotes proper tissue remodelling and reduces scar formation [70,71].

Since re-epithelialization is promoted by the proper wound cleaning and appropriate amount of granulation tissue in the early inflammatory phase of wound repair [67]. It required proliferation, differentiation, as well as migration of the endogenous stem cells [72] niched in the hair follicles and sebaceous glands [73] at the margin of the wound. This is followed by differentiation and proliferation of the epithelial cells with the presence of certain growth factors such as PDGF [22], VEGF [74], EGF, FGF [75,76] and TGF- β [35]. Such factors were provided by the activated platelets [10].

Subgroup Ia in comparison to subgroup IIa showed significant low mean value of PDGF & TGF- β in addition to the low mean area percent of VEGF. This could be attributed to the small number of activated platelets resulting into inadequate amount of granulation tissue formation and improper wound debridement. Re-epithelialization appeared in subgroup IIa but still significantly decreased than the control section. Moreover, it showed delayed appearance in the untreated group I (absent

in subgroup Ia & appeared in subgroup Ib with significant reduced thickness compared to control skin). Similar finding was demonstrated in a former study [43] where there was higher epidermal thickness 5 days following PRP treatment versus the untreated group. Despite the appearance of epidermis in subgroup Ib in the present study, skin appendages failed completely to renew. This might be linked to persistence of inflammation and the subsequent elevated IL-1 α which delayed the healing process where the uncontrollable rise in IL-1 α results in recruitment of neutrophil, tissue damage and failure of healing [22]. Further confirmation by the gross appearance at 14 days of the current study, where the wound size was noticeably reduced and covered by scar with only a small area of delayed closure.

In subgroup IIb, the epidermal thickness revealed significant increase versus subgroups Ib & IIa and non-significant decrease versus the control skin. This agrees with findings of previous research where it recorded thicker epithelium than that of untreated wound at day 14 [35]. This could be enlightened by the ability of M2 cells to produce TGF- β 1 the growth factor that promotes re-epithelialization during late inflammatory stage of wound healing [53] through proliferation as well as differentiation of the stem cells.

In subgroup IIb, PRP treatment with subsequent proper wound healing, suitable collagen deposition, & tissue remodelling, and nearly normal epidermal thickness was associated with reappearance of the skin appendages (hair follicles & sebaceous glands). Such finding is in accordance with the results detected previously in former studies where these appendages were visualized in the skin after 14 days PRP treatment of newborn mice ^[43] and diabetic wounded rats ^[35]. This finding was reported to enhance the wound healing, prevent scar formation, and complete the skin functions ^[77].

5. Conclusion:

From this study, it can be concluded that PRP could accelerate healing of full thickness wound and prevent scar formation in rats via its anti-inflammatory and angiogenic abilities. Besides, it promotes re-epithelialization, keratinocytes proliferation and proper collagen fibers deposition & arrangement.

Recommendations:

PRP can be used to promote and enhance deep wound healing and prevent scarring. Further clinical trials are recommended to evaluate the PRP application as an alternative strategy for skin wounded patients who didn't have the opportunity to graft and have a large wound area. Additional evaluation to follow-up the

healing process of PRP injection and to explore the possible side effects is recommended.

Conflict of interests:

There are no conflicts of interest.

6. References:

- 1- Biggs LC, Kim CS, Miroshnikova YA, Wickström SA. Mechanical forces in the skin: roles in tissue architecture, stability, and function. *J Invest Dermatol.* 2020; 140: 284-90.
- 2- Coates M, Blanchard S, MacLeod AS. Innate antimicrobial immunity in the skin: a protective barrier against bacteria, viruses, and fungi. *PLoS Pathog.* 2018; 14:1-7.
- 3- Iacopetti I, Perazzi A, Patruno M, Contiero B, Carolo A, Martinello T, Melotti L. Assessment of the quality of the healing process in experimentally induced skin lesions treated with autologous platelet concentrate associated or unassociated with allogeneic mesenchymal stem cells: preliminary results in a large animal model. *Front Vet Sci.* 2023; 10:1-14.
- 4- Gould L, Abadir P, Brem H, Carter M, Conner-Kerr T, Davidson J, DiPietro L, Falanga V, Fife C, Gardner S, Grice E, Harmon J, Hazzard WR, High KP, Houghton P, Jacobson N, Kirsner RS, Kovacs EJ, Margolis D, McFarland Horne F, Reed MJ, Sullivan DH, Thom S,

- Tomic-Canic M, Walston J, Whitney JA, Williams J, Zieman S, Schmader K. Chronic wound repair and healing in older adults: current status and future research. *J Am Geriatr Soc.* 2015; 63:427-38.
- 5- Nowell CS, Odermatt PD, Azzolin L, Hohnel S, Wagner EF, Fantner GE, Lutolf MP, Barrandon Y, Piccolo S, Radtke F. Chronic inflammation imposes aberrant cell fate in regenerating epithelia through mechanotransduction. *Nat Cell Biol.* 2016; 18:168-180.
- 6- Demidova-Rice TN, Hamblin MR, Herman IM. Acute and impaired wound healing: pathophysiology and current methods for drug delivery, part 1: normal and chronic wounds: biology, causes, and approaches to care. *Adv Skin Wound Care.* 2012; 25: 304-314.
- 7- Lei X, Cheng L, Yang Y, Pang M, Dong Y, Zhu X, Chen C, Yao Z, Wu G, Cheng B, Forouzanfar T. Co-administration of platelet-rich plasma and small intestinal submucosa is more beneficial than their individual use in promoting acute skin wound healing. *Burns Trauma.* 2021; 9:1-11
- 8- Alves R, Grimalt R. A Review of Platelet-Rich Plasma: History, Biology, Mechanism of Action, and Classification. *Skin Appendage Disord.* 2018; 4:18-24.
- 9- Lee KS. Ultrasound-Guided Platelet-Rich Plasma Treatment: Application and Technique. *Semin Musculoskelet Radiol.* 2016; 20:422-431.
- 10- Collins T, Alexander D, Barkatali B. Platelet-rich plasma: a narrative review. *EFORT Open Rev.* 2021; 6:225-235.
- 11- Dhurat R, Sukesh M. Principles and Methods of Preparation of Platelet-Rich Plasma: A Review and Author's Perspective. *J Cutan Aesthet Surg.* 2014; 7:189-97.
- 12- Andia I, Rubio-Azpeitia E, Martin JI, Abate M. Current Concepts and Translational Uses of Platelet Rich Plasma Biotechnology'. *Biotechnology, InTech,* 2015;1-32.
- 13- Jain NK, Gulati M. Platelet-rich plasma: a healing virtuoso. *Blood Res.* 2016; 51:3-5.
- 14- Nicoletti G, Saler M, Villani L, Rumolo A, Tresoldi MM, Faga A. Platelet Rich Plasma Enhancement of Skin Regeneration in an *ex-vivo* Human Experimental Model. *Front Bioeng Biotechnol.* 2019; 7:1-10.
- 15- Leisi S, Farahpour MR. Effectiveness of topical administration of platelet-rich plasma on the healing of methicillin-resistant *Staphylococcus aureus*-infected full-thickness wound model. *J Plast Reconstr Aesthet Surg.* 2023; 77:416-29.
- 16- Karina, Samudra MF, Rosadi I, Afini I, Widyastuti T, Sobariah S, Remelia M, Puspitasari RL, Rosliana I, Tunggadewi TI. Combination of the stromal vascular <https://ejctr.journals.ekb.eg/>

- fraction and platelet-rich plasma accelerates the wound healing process: pre-clinical study in a Sprague-Dawley rat model. *Stem Cell Investig.* 2019; 6:18.
- 17- Cavallo C, Roffi A, Grigolo B, Mariani E, Pratelli L, Merli G, Kon E, Marcacci M, Filardo G. Platelet-Rich Plasma: The Choice of Activation Method Affects the Release of Bioactive Molecules. *Biomed Res Int.* 2016; 2016:1-7.
- 18- Anushree U, Punj P, Vasumathi, Bharati S. Phosphorylated chitosan accelerates dermal wound healing in diabetic wistar rats. *Glycoconj J.* 2023; 40:19-31.
- 19- Abdollahi M, Ng TS, Rezaeizadeh A, Aamidor S, Twigg SM, Min D, McLennan SV. Insulin treatment prevents wounding associated changes in tissue and circulating neutrophil MMP-9 and NGAL in diabetic rats. *PLoS One.* 2017; 12:1-16.
- 20- Klabukov I, Yatsenko E, Baranovskii D. The effects of mesenchymal stromal cells and platelet-rich plasma treatments on cutaneous wound healing: ignoring the possibility of adverse events and side effects could compromise study results. *Arch Dermatol Res.* 2023; 316:35.
- 21- Tatar C, Aydin H, Karsidag T, Arikan S, Kabukcuoglu F, Dogan O, Bekem A, Unal A, Tuzun IS. The effects of platelet-rich plasma on wound healing in rats. *Int J Clin Exp Med.* 2017; 10:7698-7706.
- 22- Shahhosseinlou F, Farahpour MR, Sonboli A. Fabrication of novel polysaccharide hybrid nanoliposomes containing citral for targeting MRSA-infected wound healing. *J Ind Eng Chem.* 2023; 118:187–95.
- 23- Abdelmonem M, Shahin NN, Rashed LA, Amin HAA, Shamaa AA, Shaheen AA. Hydrogen sulfide enhances the effectiveness of mesenchymal stem cell therapy in rats with heart failure: In vitro preconditioning versus in vivo co-delivery. *Biomed Pharmacother.* 2019; 112:1-15.
- 24- Suvarna K, Layton C, Bancroft J. The haematoxylin and eosin, Connective and mesenchymal tissue with their stains & Immunohistochemical and immunofluorescent techniques. In *Bancroft's Theory and Practice of Histological Techniques (Eighth Edition)*, Elsevier, 2019, pp: 126-138, 153-175 & 337-394 . eBook ISBN: 9780702068867.
- 25- Han Y, Ren J, Bai Y, Pei X, Han Y. Exosomes from hypoxia-treated human adipose-derived mesenchymal stem cells enhance angiogenesis through VEGF/VEGF-R. *Int J Biochem Cell Biol.* 2019;109:59-68.
- 26- Elswaidy NR, Abd Ellatif RA, Ibrahim MAA. Ketogenic Diet Enhances Delayed Wound Healing in Immunocompromised Rats: A Histological and Immunohistochemical Study. *Egyptian* <https://ejctr.journals.ekb.eg/>

- Journal of Histology. 2022; 45:1111-1124.
- 27-Melter M, Reinders ME, Sho M, Pal S, Geehan C, Denton MD, Mukhopadhyay D, Briscoe DM. Ligation of CD40 induces the expression of vascular endothelial growth factor by endothelial cells and monocytes and promotes angiogenesis in vivo. *Blood*. 2000; 96:3801-3808.
- 28-Brown LF, Yeo KT, Berse B, Yeo TK, Senger DR, Dvorak HF, van de Water L. Expression of vascular permeability factor (vascular endothelial growth factor) by epidermal keratinocytes during wound healing. *J Exp Med*. 1992; 176:1375-1379.
- 29-Cohen I, Rider P, Vornov E, Tomas M, Tudor C, Wegner M, Brondani L, Freudenberg M, Mittler G, Ferrando-May E, Dinarello CA, Apte RN, Schneider R. IL-1 α is a DNA damage sensor linking genotoxic stress signaling to sterile inflammation and innate immunity. *Sci Rep*. 2015; 5:1-11.
- 30-Mantovani A, Dinarello CA, Molgora M, Garlanda C. Interleukin-1 and Related Cytokines in the Regulation of Inflammation and Immunity. *Immunity*. 2019; 50:778-795.
- 31-Kaneko N, Kurata M, Yamamoto T, Morikawa S, Masumoto J. The role of interleukin-1 in general pathology. *Inflamm Regen*. 2019; 39:1-16.
- 32-Juniantito V, Izawa T, Yuasa T, Ichikawa C, Yano R, Kuwamura M, Yamate J. Immunophenotypical characterization of macrophages in rat bleomycin-induced scleroderma. *Vet Pathol*. 2013; 50:76-85.
- 33-Dalmajer ES, Nord CL, Astle DE. Statistical power for cluster analysis. *BMC Bioinformatics*. 2022; 23: 205-233.
- 34-Akbarzadeh S, McKenzie MB, Rahman MM, Cleland H. Allogeneic Platelet-Rich Plasma: Is It Safe and Effective for Wound Repair? *Eur Surg Res*. 2021; 62:1-9.
- 35-Guo SC, Tao SC, Yin WJ, Qi X, Yuan T, Zhang CQ. Exosomes derived from platelet-rich plasma promote the re-epithelization of chronic cutaneous wounds via activation of YAP in a diabetic rat model. *Theranostics*. 2017; 7:81-96.
- 36-Chicharro-Alcántara D, Rubio-Zaragoza M, Damiá-Giménez E, Carrillo-Poveda JM, Cuervo-Serrato B, Peláez-Gorrea P, Sopena-Juncosa JJ. Platelet Rich Plasma: New Insights for Cutaneous Wound Healing Management. *J Funct Biomater*. 2018; 9:1-20.
- 37-Ozer K, Colak O. Leucocyte- and platelet-rich fibrin as a rescue therapy for small-to-medium-sized complex wounds of the lower extremities. *Burns Trauma*. 2019; 7: 1-9.
- 38-Karayannopoulou M, Psalla D, Kazakos G, Loukopoulos P, Giannakas N, Savvas

- I, Kritsepi-Konstantinou M, Chantes A, Papazoglou LG. Effect of locally injected autologous platelet-rich plasma on second intention wound healing of acute full-thickness skin defects in dogs. *Vet Comp Orthop Traumatol.* 2015; 28:172-178.
- 39- Xu PC, Xuan M, Cheng B. Effects and mechanism of platelet-rich plasma on military drill injury: a review. *Mil Med Res.* 2020; 7:1-7.
- 40- Rodrigues M, Kosaric N, Bonham CA, Gurtner GC. Wound Healing: A Cellular Perspective. *Physiol Rev.* 2019; 99:665-706.
- 41- Martin JM, Zenilman JM, Lazarus GS. Molecular microbiology: new dimensions for cutaneous biology and wound healing. *J Invest Dermatol.* 2010; 130:38-48.
- 42- Etulain J. Platelets in wound healing and regenerative medicine. *Platelets.* 2018; 29:556-568.
- 43- Xu P, Wu Y, Zhou L, Yang Z, Zhang X, Hu X, Yang J, Wang M, Wang B, Luo G, He W, Cheng B. Platelet-rich plasma accelerates skin wound healing by promoting re-epithelialization. *Burns Trauma.* 2020; 8:1-14.
- 44- Eo H, Lee HJ, Lim Y. Ameliorative effect of dietary genistein on diabetes induced hyper-inflammation and oxidative stress during early stage of wound healing in alloxan induced diabetic mice. *Biochem Biophys Res Commun.* 2016; 478:1021-1027.
- 45- Wynn TA, Vannella KM. Macrophages in Tissue Repair, Regeneration, and Fibrosis. *Immunity.* 2016; 44:450-62.
- 46- Dale DC, Boxer L, Liles WC. The phagocytes: neutrophils and monocytes. *Blood.* 2008; 112:935-945.
- 47- Hart J. Inflammation. 1: Its role in the healing of acute wounds. *J Wound Care.* 2002; 11:205-209.
- 48- Rodero MP, Hodgson SS, Hollier B, Combadiere C, Khosrotehrani K. Reduced Il17a expression distinguishes a Ly6c(lo)MHCII(hi) macrophage population promoting wound healing. *J Invest Dermatol.* 2013; 133:783-792.
- 49- Tabas I, Bornfeldt KE. Macrophage Phenotype and Function in Different Stages of Atherosclerosis. *Circ Res.* 2016; 118:653-667.
- 50- Larouche J, Sheoran S, Maruyama K, Martino MM. Immune Regulation of Skin Wound Healing: Mechanisms and Novel Therapeutic Targets. *Adv Wound Care (New Rochelle).* 2018; 7:209-231.
- 51- Ku CW, Yang J, Tan HY, Chan JKY, Lee YH. Decreased Innate Migration of Pro-Inflammatory M1 Macrophages through the Mesothelial Membrane Is Affected by Ceramide Kinase and Ceramide 1-P. *Int J Mol Sci.* 2022; 23:1-14.

- 52-Krzyszczczyk P, Schloss R, Palmer A, Berthiaume F. The Role of Macrophages in Acute and Chronic Wound Healing and Interventions to Promote Pro-wound Healing Phenotypes. *Front Physiol.* 2018; 9:1-22.
- 53-Chen S, Saeed AFUH, Liu Q, Jiang Q, Xu H, Xiao GG, Rao L, Duo Y. Macrophages in immunoregulation and therapeutics. *Signal Transduct Target Ther.* 2023; 8:1-35.
- 54-Lian Z, Yin X, Li H, Jia L, He X, Yan Y, Liu N, Wan K, Li X, Lin S. Synergistic effect of bone marrow-derived mesenchymal stem cells and platelet-rich plasma in streptozotocin-induced diabetic rats. *Ann Dermatol.* 2014; 26:1-10.
- 55-Marck RE, Gardien KL, Stekelenburg CM, Vehmeijer M, Baas D, Tuinebreijer WE, Breederveld RS, Middelkoop E. The application of platelet-rich plasma in the treatment of deep dermal burns: A randomized, double-blind, intra-patient controlled study. *Wound Repair Regen.* 2016; 24:712-720.
- 56-Pluthero FG, Kahr WHA. The Birth and Death of Platelets in Health and Disease. *Physiology (Bethesda).* 2018; 33:225-234.
- 57-Khalaf AA, Hassanen EI, Zaki AR, Tohamy AF, Ibrahim MA. Histopathological, immunohistochemical, and molecular studies for determination of wound age and vitality in rats. *Int Wound J.* 2019; 16:1416-1425.
- 58-Hua Y, Bergers G. Tumors vs. Chronic Wounds: An Immune Cell's Perspective. *Front Immunol.* 2019; 10:1-11.
- 59-Daley JM, Brancato SK, Thomay AA, Reichner JS, Albina JE. The phenotype of murine wound macrophages. *J Leukoc Biol.* 2010; 87:59-67.
- 60-Shook B, Xiao E, Kumamoto Y, Iwasaki A, Horsley V. CD301b+ Macrophages Are Essential for Effective Skin Wound Healing. *J Invest Dermatol.* 2016; 136:1885-1891.
- 61-Sawaya AP, Stone RC, Brooks SR, Pastar I, Jozic I, Hasneen K, O'Neill K, Mehdizadeh S, Head CR, Strbo N, Morasso MI, Tomic-Canic M. Deregulated immune cell recruitment orchestrated by FOXM1 impairs human diabetic wound healing. *Nat Commun.* 2020; 11:1-14.
- 62-Archer NK, Jo JH, Lee SK, Kim D, Smith B, Ortines RV, Wang Y, Marchitto MC, Ravipati A, Cai SS, Dillen CA, Liu H, Miller RJ, Ashbaugh AG, Uppal AS, Oyoshi MK, Malhotra N, Hoff S, Garza LA, Kong HH, Segre JA, Geha RS, Miller LS. Injury, dysbiosis, and filaggrin deficiency drive skin inflammation through keratinocyte IL-1 α release. *J Allergy Clin Immunol.* 2019; 143:1-33
- 63-Wang X, Bove AM, Simone G, Ma B. Molecular Bases of VEGFR-2-Mediated Physiological Function and Pathological Role. *Front Cell Dev Biol.* 2020; 8:1-12.

- 63- Yu C, Xu ZX, Hao YH, Gao YB, Yao BW, Zhang J, Wang B, Hu ZQ, Peng RY. A novel microcurrent dressing for wound healing in a rat skin defect model. *Mil Med Res.* 2019; 6:1-9.
- 64- Zhang J, Luo Q, Hu Q, Zhang T, Shi J, Kong L, Fu D, Yang C, Zhang Z. An injectable bioactive dressing based on platelet-rich plasma and nanoclay: Sustained release of deferoxamine to accelerate chronic wound healing. *Acta Pharm Sin B.* 2023; 13:4318-4336.
- 65- Zhang X, Yao D, Zhao W, Zhang R, Yu B, Ma G, Li Y, Hao D, Xu FJ. Engineering platelet-rich plasma based dual-network hydrogel as a bioactive wound dressing with potential clinical translational value. *Adv Funct Mater.* 2021; 31:1-14.
- 66- Alhajj M, Goyal A. Physiology, Granulation Tissue. 2022 Oct 24. In: StatPearls [Internet]. Treasure Island (FL): StatPearls Publishing; 2024 Jan-. PMID: 32119289.
- 67- Zhang L, Hu C, Xu W, Wu D, Lei S. Advances in wound repair and regeneration: Systematic comparison of cell free fat extract and platelet rich plasma. *Front Chem.* 2022; 10:1-10.
- 68- Morgan NH, Abouelgoud M, Haiba DA, Arakeep HM. Comparative Study on the Effect of Injectable Platelet Rich Plasma versus its Topical Application in the Treatment of Thermal Burn in Adult Male Albino Rat: Histological and Immunohistochemical Study. *Egyptian Journal of Histology.* 2022; 45:125-135.
- 69- Zeng XL, Sun L, Zheng HQ, Wang GL, Du YH, Lv XF, Ma MM, Guan YY. Smooth muscle-specific TMEM16A expression protects against angiotensin II-induced cerebrovascular remodeling via suppressing extracellular matrix deposition. *J Mol Cell Cardiol.* 2019; 134:131-143.
- 70- Yang L, Witten TM, Pidaparti RM. A biomechanical model of wound contraction and scar formation. *J Theor Biol.* 2013; 332:228-248.
- 71- Li Y, Zhang J, Yue J, Gou X, Wu X. Epidermal Stem Cells in Skin Wound Healing. *Adv Wound Care (New Rochelle).* 2017; 6:297-307.
- 72- Díaz-García D, Filipová A, Garza-Veloz I, Martinez-Fierro ML. A Beginner's Introduction to Skin Stem Cells and Wound Healing. *Int J Mol Sci.* 2021; 22:1-20.
- 73- Gong L, Xiao J, Li X, Li Y, Gao X, Xu X. IL-36 α Promoted Wound Induced Hair Follicle Neogenesis via Hair Follicle Stem/Progenitor Cell Proliferation. *Front Cell Dev Biol.* 2020; 8:1-11.
- 74- Eming SA, Martin P, Tomic-Canic M. Wound repair and regeneration: mechanisms, signaling, and translation. *Sci Transl Med.* 2014; 6:1-36.

- 75- Portou MJ, Baker D, Abraham D, Tsui J. The innate immune system, toll-like receptors and dermal wound healing: A review. *Vascul Pharmacol.* 2015; 71:31-36.
- 76- Wu LW, Chen WL, Huang SM, Chan JY. Platelet-derived growth factor-AA is a substantial factor in the ability of adipose-derived stem cells and endothelial progenitor cells to enhance wound healing. *FASEB J.* 2019; 33:2388-2395.
- 77- Weng T, Wu P, Zhang W, Zheng Y, Li Q, Jin R, Chen H, You C, Guo S, Han C, Wang X. Regeneration of skin appendages and nerves: current status and further challenges. *J Transl Med.* 2020; 18:1-17.